http://dx.doi.org/10.5012/bkcs.2014.35.11.3299

Indium Sulfide and Indium Oxide Thin Films Spin-Coated from Triethylammonium Indium Thioacetate Precursor for *n*-Channel Thin Film Transistor

Tung Duy Dao and Hyun-Dam Jeong*

Department of Chemistry, Chonnam National University, Gwangju-si 500-575, Korea
**E-mail: hdjeong@chonnam.ac.kr*
Received April 18, 2014, Accepted July 30, 2014

The In_2S_3 thin films of tetragonal structure and In_2O_3 films of cubic structure were synthesized by a spin coating method from the organometallic compound precursor triethylammonium indium thioacetate ($[(Et)_3NH]^+[In(SCOCH_3)_4]^-$; TEA-InTAA). In order to determine the electron mobility of the spin-coated TEA-InTAA films, thin film transistors (TFTs) with an inverted structure using a gate dielectric of thermal oxide (SiO_2) was fabricated. These devices exhibited *n*-channel TFT characteristics with a field-effect electron mobility of 10.1 $cm^2V^{-1}s^{-1}$ at a curing temperature of 500 °C, indicating that the semiconducting thin film material is applicable for use in low-cost, solution-processed printable electronics.

Key Words : Indium sulfide, Indium oxide, Thioacetate, Spin coating, Thin film transistor

Introduction

Indium sulfide (In_2S_3) is an n-type III-VI semiconductor which has shown many important optoelectronic,[1-3] photoconductive,[4] and optical properties,[1,5,6] which subsequently inspired applications for use in the preparation of phosphors for color televisions[7,8] and heterojunctions for photovoltaic electric generators.[9] Meanwhile, In_2O_3 is another important member of the n-type III-VI semiconductor family, which has low resistivity, a low absorbance in the visible region, and a high infrared light reflectivity.[10,11] Solution-processed thin-film deposition methods, such as spin-coating, could offer many advantages, such as low cost and high throughput, enabling the fabrication of high-performance and low-cost electronics. In this studying, we focus on the spin-coating of the organometallic precursor, triethylammonium indium thioacetate ($[(Et)_3NH]^+ [In(SCOCH_3)_4]^-$; TEA-InTAA), which is supposed to proceed in a condensation reaction to form an In_2S_3 network at a relatively low curing temperature (200 ÷ 400 °C), and an In_2O_3 network at high curing temperature (500 ÷ 600 °C). In order to determine the electron mobility (μ) of the spin-coated TEA-InTAA films, thin film transistors (TFTs) with an inverted structure using a gate dielectric of thermal oxide (SiO_2) was fabricated, as shown in Scheme 1. These devices exhibited *n*-channel TFT characteristics with a field-effect electron mobility of 10.1 $cm^2V^{-1}s^{-1}$ at a curing temperature of 500 °C, indicating that the semiconducting thin film material is applicable for use in low-cost, solution-processed printable electronics.

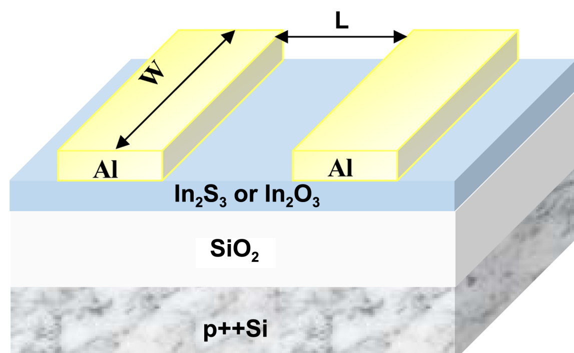

Scheme 1. Thin film transistor (TFT) with an inverted structure, having a gate dielectric of thermal oxide (SiO_2), where the semiconducting channel layer is fabricated *via* a spin coating process from an organometallic precursor, triethylammonium indium thioacetate (TEA-InTAA). The channel width (W) and length (L) are 1000 μm and 100 μm, respectively.

Experimental

Materials. All reagents were supplied by Aldrich Chemical Co. (St. Louis, MO, USA): thioacetic acid (CH_3COSH, 96%), potassium thioacetate ($KS(CO)CH_3$), Indium chloride ($InCl_3$), triethylamine ($(Et)_3N$), the solvents methylene chloride (MC) and acetone nitride.

Synthesis of TEA-InTAA Organometallic Precursor. The organometallic precursor, triethylammonium indium thioacetate ($[(Et)_3NH]^+ [In(SCOCH_3)_4]^-$; TEA-InTAA), was synthesized following the procedure described by J.Vittal's Group[12] with small modifications. Indium thioacetate was synthesized by mixing 0.25 mmol of $InCl_3$ and 0.25 mmol of $KS(CO)CH_3$ in 15 mL of water, stirring for 1 h. Triethylammonium thioacetate was synthesized by the reaction of 0.25 mmol of $(Et)_3N$ with 0.75 mmol of CH_3COSH in MC solvent. The triethylamonium thioacetate solution was added in drops to Indium thioacetate, and stirred for over 2 h. After reaction, the solution was separated by extraction to get the organic layer, which was concentrated by rotary evaporation to get the resin. This resin was washed by petroleum ether and diethyl ether several times to obtain a light yellow powder, TEA-InTAA organometallic precursor.

Fabrication of TEA-InTAA Thin Films. 10 wt % solution

of the TEA-InTAA organometallic precursor in acetone nitride was spin-coated on Si(100) wafer at 500 rpm for 5 seconds, then 2000 rpm for 25 seconds. Next, the films were cured at 200 °C, 300 °C, 400 °C, 500 °C and 600 °C for 2 h in a furnace, these films will use for XRD investigation.

Fabrication of TEA-InTAA Thin Film Transistor (TFT) Devices. TFTs of inverted structure were employed with a thermal oxide (SiO_2) gate dielectric layer, and heavily doped p-type Si wafer as the gate electrode, as shown in Scheme 1. 10 wt % solution of the TEA-InTAA organometallic precursor in acetone nitride was spin-coated on the SiO_2/Si wafer at 500 rpm for 5 seconds, then 2000 rpm for 25 seconds. Next, the films were cured at high temperatures in a furnace at 200 °C, 300 °C, 400 °C, 500 °C and 600 °C for 2 h, like the treatment for the XRD investigation. And then, the films were deposited Al electrodes to construct TFT devices.

Materials Characterization. Fourier-transform infrared spectroscopy (FT-IR) was performed using a PerkinElmer (Waltham, Massachusetts, USA) spectrometer with a resolution of 8 cm^{-1}. A superconducting FT-NMR 300 MHz (Varian, Inc, Paolo, Alto, California, USA) was used to measure ^{1}H-NMR spectra of TEA-InTAA precursor. Thermogravimetric analysis (TGA) was conducted on a METTLER TOLEDO SDTA851e under N_2 flow from room temperature to 900 °C. X-ray diffraction (XRD) spectra of the TEA-InTAA thin films were obtained using an X'Pert Pro Multi Purpose X-ray diffractometer (PANalytical, Almelo, Nerthelands) equipped with a Cu Kα source operated at 40 kV and 30 mA. The 2θ angle was scanned from 10 to 90 degrees at an increasing rate of 2 degrees per min and step size of 0.05 degrees. Thin film transistor (TFT) characteristics were obtained in air atmosphere at room temperatures using a HP 4145B semiconductor parameter analyzer.

Results and Discussion

Fourier transform infrared (FT-IR) spectroscopy was performed on the synthesized powder of TEA-InTAA, as shown in Figure 1. The peaks around 2800 ÷ 3200 cm^{-1} are attributed to the amine group of the triethylammonium cation. The strong peaks around 1100 ÷ 1600 cm^{-1} are due to the stretching vibration of the carbonyl group of the thioacetate (TAA; $CH_3C(=O)S$) ligands. In the range of 1000 ÷ 500 cm^{-1}, the first two peaks at 950 cm^{-1} and 840 cm^{-1} are due to C=S stretching vibration in the TAA resonance structure, and the later 624 cm^{-1} peak is attributed to the C-S stretching vibration in the In–S-C(=O) bond, where the sulfur atom is covalently bonded to the In element of the organometallic compound.[12]

The molecular structure of the $[(Et)_3NH]^+[In(SCOCH_3)_4]^-$ precursor was further confirmed by nuclear magnetic resonance (NMR) spectroscopy, as shown in Figure S1 (supplementary materials).

From the thermogravimetric analysis (TGA) result of the precursor (supplementary materials), a thermal decomposition reaction occurred at about 200 °C, while the condensation reaction occurred to give rise to the –In-S-In– linkage

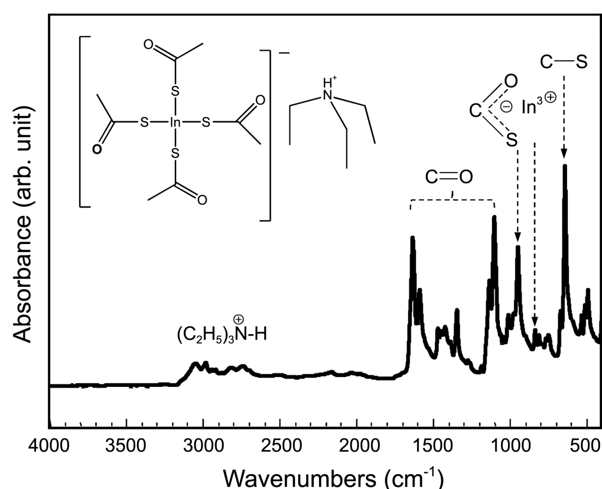

Figure 1. FT-IR of the $[(Et)_3NH]^+[In(SCOCH_3)_4]^-$ organometallic precursor.

and thioacetic anhydride ($CH_3C(=O)SC(=O)CH_3$) (Reaction R1).

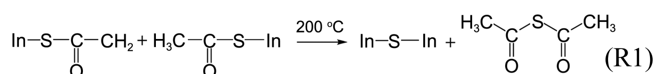

(R1)

This condensation mechanism has already been proposed in the previous studies for thioacetic acid capped InP quantum dots,[13] thioacetic acid capped PbS quantum dots,[14] and solution-processed CdS thin films.[15]

The thermal evolution of the crystalline phase in the spin-coated films was investigated from their X-ray diffraction (XRD) spectra (Figure 2). Films were fabricated by a curing process at 200 °C, 300 °C, 400 °C, 500 °C and 600 °C for 2 hours in a furnace, after spin-coating the TEA-InTAA precursor solution on Si(100) wafer. The thin films cured at 200 °C and 300 °C show no peaks in the XRD spectra, even though the condensation reaction making In-S network structure surely proceeds as explained in the TGA results. At 400 °C, the amorphous In-S network structure changes to

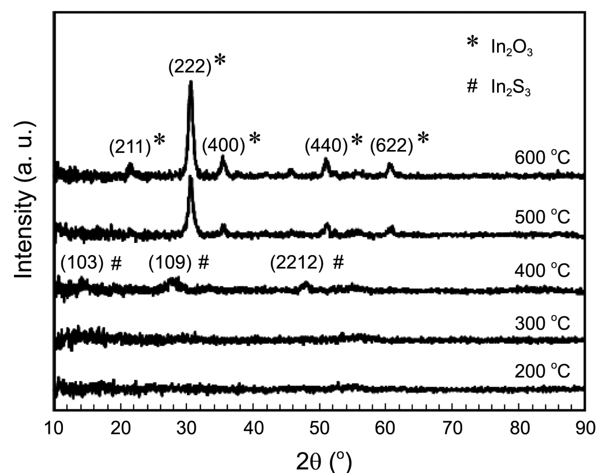

Figure 2. XRD spectra for the $[(Et)_3NH]^+[In(SCOCH_3)_4]^-$ complex: thin film at different curing temperatures.

form the tetragonal structure of the In_2S_3 crystalline phase, confirmed by the peaks of In_2S_3 (103, 109, and 2212) (Figure 2), where the estimated lattice parameter of a = 7.74 Å and c = 32.1 Å were close to the reported values (JCPDS card no. 25-0390, a = 7.8 Å and c = 33.1 Å) for pure tetragonal In_2S_3 phase.[16] At higher curing temperatures of 500 °C and 600 °C, the tetragonal In_2S_3 phase was oxidized to In_2O_3, which was confirmed by the appearance of peaks corresponding to the cubic structure of In_2O_3 (211, 222, 400, 440, and 622) , where the estimated lattice constant value a = 10.13 Å was also in good agreement with the reported value of a = 10.118 Å (JCPDS card no. 06-0416).[16] The oxidation reaction for the phase conversion of tetragonal In_2S_3 to cubic In_2O_3 is expressed in Reaction R2. Thermodynamic calculations revealed that at both 500 °C and 600 °C, the Gibb free energy (ΔG°) of the reaction is largely negative; that is, the phase transformation reaction from In_2S_3 to In_2O_3 is spontaneous.[16]

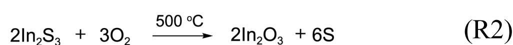

$$2In_2S_3 + 3O_2 \xrightarrow{500\,^{\circ}C} 2In_2O_3 + 6S \quad \text{(R2)}$$

To measure the field-effect mobilities (μ) of the spin-coated TEA-InTAA films, TFTs of inverted structure were employed with a thermal oxide (SiO_2) gate dielectric layer, and heavily doped p-type Si wafer as the gate electrode, as shown in Scheme 1. Representative plots of the drain current (I_{DS}) *versus* the drain voltage (V_{DS}) are shown in Figure 3(a) for various applied gate voltages (V_G) for a sample cured at 500 °C, which followed the behavior of n type field effect transistor. Those for the other curing temperatures are shown in the supplementary materials. A transfer curve with drain current (I_{DS}) plotted as a function of V_G is shown in Figure 3(b) for a V_{DS} of 40 V in the pseudo-saturation region of the sample cured at 500 °C. From the linear fits in Figure 3(b), the field-effect mobility (μ), in the saturation regime was determined with the following equation, from the conventional metal-oxide-metal semiconductor field-effect transistor model:[17]

$$I_{DS} = \frac{WC_i\mu}{2L}(V_G - V_T)^2 \quad (1)$$

C_i is the areal capacitance of the SiO_2 gate insulator, W is the channel width, L is the channel length, V_T is the threshold voltage, and μ the field-effect mobility. The field effect mobility under saturation conditions (μ_{sat}) was then calculated from the slope of the plot of $I_{DS}^{1/2}$ *versus* V_{GS}. From the data in Figure 3(b), a field-effect mobility in the saturation region (μ_{sat}) of 10.1 $cm^2V^{-1}s^{-1}$, a threshold voltage of −54 V, and an on/off current ratio (I_{on}/I_{off}) of 28.17 were obtained.

In a similar way, μ_{sat} and I_{on}/I_{off} values were also calculated for the TFT devices of the thin films cured at 200 °C, 300 °C, 400 °C, and 600 °C, as summarized in Table 1. At a curing temperature of 200 °C and 300 °C, the In_2S_3 network structure has difficulty obtaining mobility. At a curing temperature of 400 °C, In_2S_3 thin films of tetragonal structure show low μ_{sat} values. However, at higher curing temperatures of 500 °C and 600 °C, the In_2S_3 phase was oxidized to the In_2O_3 phase with a large increase in μ_{sat}, which may be due to different structural material. But the 600 °C cured sample has poorer μ_{sat} and I_{on}/I_{off} value than 500 °C cured one. We think this is attributed to the fact that Reaction R2 at 600 °C is faster than that at 500 °C. Thus, phase conversion rate from the In_2S_3 to In_2O_3 was increased with increase in the amount of sulfur formed in the semiconductor phase at an elevated curing temperature of 600 °C. This process may

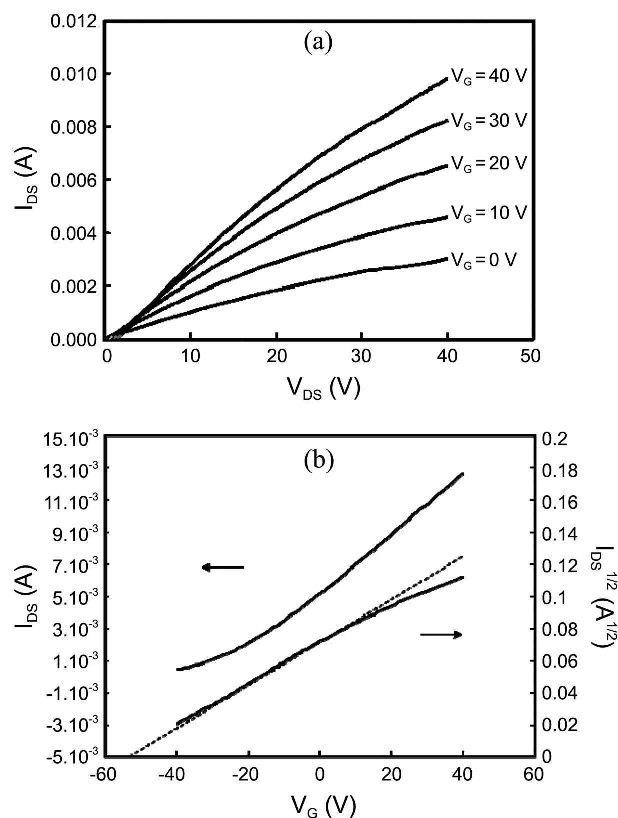

Figure 3. TFT properties of $[(Et)_3NH]^+[In(SCOCH_3)_4]^-$ organometallic thin film cured at 500 °C. (a) Output characteristics: I_{DS} *versus* V_{DS} for various V_{GS}. (b) Transfer characteristics: I_{DS} *versus* V_{GS} for constant V_{DS} (V_{DS} = 40 V).

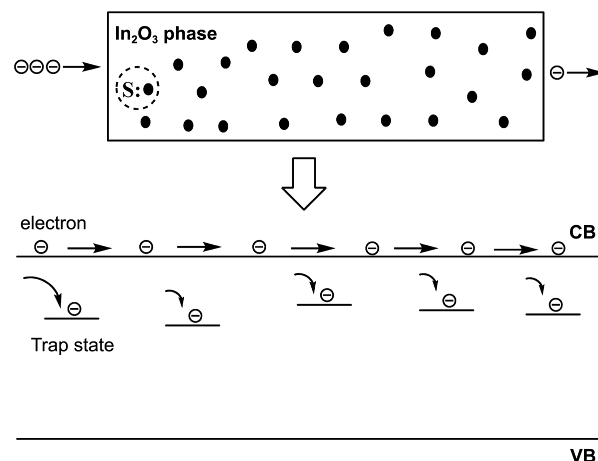

Scheme 2. Electron transport model for the formation of trap states due to sulfur phases in In_2O_3 crystal thin film.

Table 1. Mobility values in the saturation (μ_{sat}) and on/off current ratio (I_{on}/I_{off}) for the TFT devices of the thin films, according to the curing temperatures

Curing temperature (°C)	μ_{sat} ($cm^2V^{-1}s^{-1}$)	I_{on}/I_{off}
200	–	–
300	7.50×10^{-6}	4.57
400	2.40×10^{-5}	2.15
500	1.01×10^{-1}	28.17
600	4.75×10^{-1}	4.45

induce the trap states in the semiconductor phase, particularly, at the interface between In_2O_3 and sulfur phases. We suggest the reason why the 600 °C cured sample has poorer μ_{sat} and I_{on}/I_{off} value than 500 °C cured one is due to an increased carrier scattering associated with increased trap states as the curing temperature is increased. The same trend was also found in solution-processed ZnO.[18] A model for explaining such a situation is given in Scheme 2, trap states are created from interface between In_2O_3 and S phase. While electrons are moving in conduction band (CB) of In_2O_3 phase, they can be trapped on trap states.

We obtained high mobility (10.1 $cm^2V^{-1}s^{-1}$) from the In_2O_3 thin film cured at 500 °C. Compared to the device performance of the recently reported metal oxide TFTs (ZnO, ZTO, IZO, IZTO, AIO, GIZO oxide semiconductors) with a field-effect mobility smaller than 10 $cm^2V^{-1}s^{-1}$,[19] our result is significantly improved. The mobility of our In_2O_3 TFT (10.1 $cm^2V^{-1}s^{-1}$) is also better than that of the printed In_2O_3 TFT with mobility of 6 $cm^2V^{-1}s^{-1}$.[20]

In summary, the In_2S_3 thin films of tetragonal structure and In_2O_3 films of cubic structure were synthesized by a spin coating method from the organometallic compound precursor triethylammonium indium thioacetate ($[(Et)_3NH]^+$-$[In(SCOCH_3)_4]^-$; TEA-InTAA). A high field effect electron mobility of 10.1 $cm^2V^{-1}s^{-1}$, which was obtained using TFT devices, was observed for the cubic In_2O_3 film cured at 500 °C.

Conclusion

In summary, the In_2S_3 thin films of tetragonal structure and In_2O_3 films of cubic structure were synthesized by a spin coating method from the organometallic compound precursor triethylammonium indium thioacetate ($[(Et)_3NH]^+$-$[In(SCOCH_3)_4]^-$; TEA-InTAA). A high field effect electron mobility of 10.1 $cm^2V^{-1}s^{-1}$, which was obtained using TFT devices, was observed for the cubic In_2O_3 film cured at 500 °C.

Acknowledgments. This work was supported by the Materials Original Technology Program (10041222) funded by the Ministry of Knowledge Economy (MKE, Korea).

Supplementary Materials. Supplementary materials is available.

References

1. Kim, W. T.; Kim, C. D. *J. Appl. Phys*. **1986**, *60*, 2631.
2. Nomura, R.; Inazawa, S.; Kanaya, K.; Matsuda, H. *Appl. Organomet. Chem.* **1989**, *3*, 195.
3. Asikainen, T.; Ritala, M.; Leskela, M. *Appl. Surf. Sci*. **1994**, *82/83*, 122.
4. Dalas, E.; Kobotiatis, L. *J. Mater. Sci*. **1993**, *28*, 5456.
5. Diehl, R.; Nitsche, R. *J. Cryst. Growth.* **1975**, *28*, 306.
6. Choe, S. H.; Band, T. H.; Kim, N. O.; Kim, H. G.; Lee, C. I.; Jin, M. S.; Oh, W. T.; Kim, W. T. *Semicond. Sci. Technol.* **2001**, *16*, 98.
7. Takeshi, T.; Susumu, M.; Toshio, N.; Nobuo, I. *Japanese Patent Application; Chem. Abstr*. **1979**, *91*, 67384a. Patent Application No: 77/139,889.
8. Toshiba Corp. *Japanese Patent Application; Chem. Abstr*. **1979**, *96*, 113316h. Patent Application No: 80/57764.
9. Dalas, E.; Sakkopoulos, S.; Vitoratos, E.; Maroulis, G. *J. Mater. Sci.* **1993**, *28*, 5456.
10. Hamberg, I.; Granqvist, C. G. *J. Appl. Phys.* **1986**, *60*, R123.
11. Zhang, Y.; Jia, H.; Yu, D.; Luo, X.; Zhang, Z.; Chen, X. *J. Mater. Res.* **2003**, *18*, 2793.
12. Deivaraj, T. C.; Lin, M.; Loh, K. P.; Yeadon, M.; Vittal, J. J. *J. Mater. Chem.* **2003**, *13*, 1149.
13. Dung, M. X.; Tung, D. D.; Jeong, H. D. *Curr. Appl. Phys*. **2013**, *13*, 1075
14. Dao, T. D.; Hafez, M. E.; Beloborodov, I. S.; Jeong, H. D. *Bull. Korean Chem. Soc*. **2014**, *35*, 457.
15. Seon, J. B.; Lee, S.; Kim, J. M.; Jeong, H. D. *Chem. Mater*. **2009**, *21*, 604.
16. Datta, A.; Panda, S. K.; Ganguli, D.; Mishra, P.; Chaudhuri, S. *Crystal Growth & Design* **2007**, *7*, 163.
17. Shekar, B. C.; Lee, J.; Rhee, S. W. *Korean J. Chem. Eng*. **2004**, *21*, 267.
18. Li, C. S.; Li, Y. N.; Wu, Y. L.; Ong, B. S.; Loutfy, R. O. *J. Mater. Chem*. **2009**, *19*, 1626.
19. Fortunato, N.; Barquinha, P.; Martins, R. *Adv. Mater*. **2012**, *24*, 2945.
20. Kim, M. G.; Kanatzidis, M. G.; Facchetti, A.; Marks, T. J. *Nature Materials* **2011**, *10*, 382.